Biophysical Chemistry 158 (2011) 111–118

Contents lists available at ScienceDirect

Biophysical Chemistry

journal homepage: http://www.elsevier.com/locate/biophyschem

Thermodynamic properties and characterization of proteoliposomes rich in microdomains carrying alkaline phosphatase

M. Bolean [a], A.M.S. Simão [a], B.Z. Favarin [a], J.L. Millán [b], P. Ciancaglini [a,*]

[a] Depto. Química, Faculdade de Filosofia, Ciências e Letras de Ribeirão Preto da Universidade de São Paulo (FFCLRP-USP), Ribeirão Preto, SP, Brazil
[b] Sanford Children's Health Research Center, Sanford–Burnham Medical Research Institute, La Jolla, CA, USA

ARTICLE INFO

Article history:
Received 28 March 2011
Received in revised form 18 May 2011
Accepted 21 May 2011
Available online 27 May 2011

Keywords:
Alkaline phosphatase
Differential Scanning Calorimetry (DSC)
Cholesterol
Ganglioside
Microdomain
Sphingolipid

ABSTRACT

Tissue-nonspecific alkaline phosphatase (TNAP) is associated to the plasma membrane via a GPI-anchor and plays a key role in the biomineralization process. In plasma membranes, most GPI-anchored proteins are associated with "lipid rafts", ordered microdomains enriched in sphingolipids, glycosphingolipids and cholesterol. In order to better understand the role of lipids present in rafts and their interactions with GPI-anchored proteins, the insertion of TNAP into different lipid raft models was studied using dipalmitoylphosphatidylcholine (DPPC), cholesterol (Chol), sphingomyelin (SM) and ganglioside (GM1). Thus, the membrane models studied were binary systems (9:1 molar ratio) containing DPPC:Chol, DPPC:SM and DPPC:GM1, ternary systems (8:1:1 molar ratio) containing DPPC:Chol:SM, DPPC:Chol:GM1 and DPPC:SM:GM1 and finally, a quaternary system (7:1:1:1 molar ratio) containing DPPC:Chol:SM:GM1. Calorimetry analysis of the liposomes and proteoliposomes indicate that lateral phase segregation could be noted only in the presence of cholesterol, with the formation of cholesterol-rich microdomains centered above Tc = 41.5 °C. The presence of GM1 and SM into DPPC-liposomes influenced mainly ΔH and $\Delta t_{1/2}$ values. The gradual increase in the complexity of the systems decreased the activity of the enzyme incorporated. The presence of the enzyme also fluidifies the systems, as seen by the intense reduction in ΔH values, but do not alter Tc values significantly. Therefore, the study of different microdomains and its biophysical characterization may contribute to the knowledge of the interactions between the lipids present in MVs and its interactions with TNAP.

1. Introduction

Many studies referring to the participation of tissue-nonspecific alkaline phosphatase (TNAP) during the calcification process have demonstrated the existence of two forms of the enzyme: membrane-bound and soluble TNAP. Although there are controversies related to the physiological role of TNAP, only the membrane-bound enzyme has been associated with the mineralization process [1–9].

TNAP is attached to the cell membrane via a glycosylphosphatidylinositol (GPI) anchor. This anchor structure results in lateral mobility of the enzyme in the membrane, accumulation of the enzyme in specific microenvironments, as well as the release of the protein from the membrane by phospholipase C (specific to phosphatidylinositol) in a highly controlled manner [5,7,10].

Recent studies have proposed that a primary role of TNAP in the bone matrix is to restrict the concentration of extracellular inorganic pyrophosphate (PPi), a potent mineralization inhibitor, to maintain a Pi/PPi ratio permissive for normal bone mineralization [7,11–14]. TNAP is also a potent ATPase at the level of matrix vesicles (MVs) [12]. Furthermore, recent data suggest that the location of TNAP on the membrane of MVs plays a role in determining substrate selectivity in this microcompartment [6,13,14].

Given the crucial role of TNAP in the biomineralization process, the significance of MV for skeletal mineralization and the observations that the lipidic composition of MVs changes as mineralization proceeds, it is essential to understand the interrelationship of GPI-anchored TNAP and the lipidic components of the MV membrane [15].

It is important note that lipids are not distributed randomly in biological membranes. Glycosphingolipids (cerebrosides and gangliosides), which typically contains long chains of saturated fatty acids, form transitory aggregates at the external lamella that excludes glycerophospholipids, which typically contains an unsaturated fatty acyl group and a saturated fatty acyl group of smaller length. The long saturated acyl groups of sphingolipids can form more stable and compact associations with the rings of the cholesterol structure than the shorter and generally unsaturated chains of phospholipids, forming what is called "lipid rafts" [16]. The organization of biological membranes into microdomains is believed to play a key role in several cellular processes such as protein targeting and signal transduction [17]. The existence of these microdomains is explained mainly by the

* Corresponding author at: Depto Química, FFCLRP-USP; Av. Bandeirantes, 3900, 14040-901; Ribeirão Preto, SP, Brazil. Tel.: +55 16 36023753; fax: +55 16 36024838.
E-mail address: pietro@ffclrp.usp.br (P. Ciancaglini).

0301-4622/$ – see front matter © 2011 Elsevier B.V. All rights reserved.
doi:10.1016/j.bpc.2011.05.019

lateral phase separation of membrane lipids in a fluid liquid crystalline phase (Lα) and a liquid ordered phase (Lo) rich mostly in cholesterol and sphingolipids [18–20]. It was proposed that these lipid aggregates occur at the surface of the membrane driven only by distinctive intermolecular interactions, including van der Waals interactions between the long, nearly fully saturated chains of sphingomyelin and glycosphingolipids as well as hydrogen bonding between adjacent glycosyl moieties of glycosphingolipids [21]. These interactions may explain the existence of certain lipid compositions resistant to solubilization by detergents, particularly those containing sphingomyelin, cholesterol, glycosphingolipids and saturated phospholipids [22]. According to the lipid rafts hypothesis and the evolution of this concept, rafts would be small transient microdomains enriched with peculiar lipids, together with specific proteins, that would have a role in cellular functions such as intracellular lipid traffic and cell signaling. This definition explains the inhomogeneous distribution of membrane proteins by a spontaneous de-mixing of lipids to form different domains with different properties and, thus, different environments for certain membrane proteins [20,23].

In plasma membranes, two classes of proteins would be associated with lipid rafts: proteins anchored to the membrane by two long chains of saturated fat acid linked covalently (two palmitoyl groups or one palmitoyl group and one miristoyl group) and GPI-anchored proteins, as is the case of TNAP. Probably, lipid anchors, as occurs with acyl chains of sphingolipids, form more stable associations with cholesterol and with the long acyl groups in lipid rafts, than with the surrounding phospholipids [24]. Moreover, GPI-anchored proteins would also be concentrated in detergent resistant membranes (DRM), Triton X-100-resistant membrane complexes (TRMC), detergent-insoluble glycolipid-enriched fraction (DIG) or glycosphingolipid-enriched membranes (GEM) [20,21,25,26].

A number of different biophysical techniques, e.g. Atomic Force Microscopy, Fluorescence Microscopy, Differential Scanning Calorimetry (DSC), Spin-label electron resonance spectroscopy, and others [21,22,26,27] have been applied to the characterization of lipid microdomains. These microdomains may occupy up to 50% of membrane surface, are slightly thicker and more ordered (less fluid) than the surrounding microdomains rich in phospholipids, being more difficult to solubilize by neutral detergents. They behave as "rafts" of ordered liquid sphingolipids in an ocean of disordered liquid phospholipids [28].

The microdomains present in membranes are not strictly separated and the proteins can move in a time scale of seconds. However, in a time scale of microseconds (more relevant for many biochemical processes mediated by enzymes and membranes), many proteins reside preferentially in the rafts [24]. So, studies with these systems are essential to understanding the mechanisms of action of TNAP in lipid interfaces.

We recently studied a mimetic system containing only DPPC and cholesterol and showed that the gradual proportional increase of cholesterol in liposomes results in broadening of the phase transition peak and the formation of microdomains [17]. Thus, enzyme incorporation influences cooperativity and induces further changes in calorimetric enthalpy by affecting lipid–lipid interactions. Here we report the production of biomimetic systems with microdomains for the incorporation of TNAP.

2. Materials and methods

2.1. Materials

All aqueous solutions were made using Millipore DirectQ ultra pure apyrogenic water. Bovine serum albumin (BSA), Tris hydroxymethyl-amino-methane (Tris), 2-amino-2-methyl-propan-1-ol (AMPOL), sodium dodecylsulfate (SDS), p-nitrophenyl phosphate disodium salt (PNPP), dexamethasone, glucose 1-phosphate, glucose 6-phosphate, fructose 6-phosphate, β-glycerophosphate, polyoxyethylene-9-lauryl ether (polidocanol), α-naphthyl phosphate, Fast Blue RR, dipalmitoyl-phosphatidylcholine (DPPC) MW = 734.1 $g \cdot mol^{-1}$, cholesterol (Chol) MW = 386.65 $g \cdot mol^{-1}$, sphingomyelin (SM) MW = 731.09 $g \cdot mol^{-1}$, from bovine brain ≥ 97.0% pure, ganglioside (GM1) of type III, purified from bovine brain, MW = 1563.88 $g \cdot mol^{-1}$, were from Sigma Chemical Co. (St Louis, MO, USA); sodium chloride and magnesium chloride were from Merck (São Paulo, SP, Brazil). 75 cm^2 plastic culture flasks were from Corning (Cambridge, MA, USA). α-MEM, fetal bovine serum, ascorbic acid, gentamicin and fungizone were from Gibco-Life Technologies (Grand Island, NY, USA). Analytical grade reagents were used without further purification.

2.2. Rat bone marrow cell isolation and culture

Cells were prepared and cultured according to Simão et al. [13]. Bone marrow was obtained from young adult male rats of the Wistar strain weighing 110–120 g. The femora were excised aseptically, cleaned of soft tissues, and washed 3 times, 15 min each in culture medium containing 10 times the usual concentration of antibiotics (see below). The epiphyses of femora were cut off and the marrow flushed out with 20 mL of culture medium. Bone marrow cells released were collected in a 75 cm^2 plastic culture flask containing 10 mL of culture medium composed by α-MEM, supplemented with 15% fetal bovine serum, 50 $\mu g \cdot mL^{-1}$ gentamicin, 0.3 $\mu g \cdot mL^{-1}$ fungizone, 10^{-7} M dexamethasone, 5 $\mu g \cdot mL^{-1}$ ascorbic acid and 2.16 $mg \cdot mL^{-1}$ β-glycerophosphate. Cells were cultured for 14 days at 37 °C in a humidified atmosphere of 5% CO_2 and 95% air, and the medium was changed every 48 h. The cultures were observed and evaluated under an inverted phase microscope after 24 h, 4 days, 10 days and 14 days.

2.3. Preparation of membrane-bound alkaline phosphatase

Membrane-bound alkaline phosphatase, an osteoblast-specific marker, was prepared from cell culture as described by Simão et al. [13]. The cells were washed with 50 mM Tris–HCl buffer, pH 7.5, containing 2 mM $MgCl_2$, removed with a spatula and resuspended in 50 mM Tris–HCl buffer, pH 7.5, containing 10 mM $MgSO_4$ and 0.8 M NaCl (osmotic buffer).

The cell suspension was homogenized using a "potter system" for gentle cell disruption, at 4 °C for 15 min, centrifuged at 1000×*g* for 3 min and finally the supernatant was centrifuged at 100,000×*g* for 1 h at 4 °C. The pellet corresponding to membrane bound alkaline phosphatase, was resuspended in 50 mM Tris–HCl buffer, pH 7.5, containing 2 mM $MgCl_2$, frozen in liquid nitrogen and stored at −20 °C.

2.4. Estimation of protein

Protein concentrations were estimated according to Hartree [29] in the presence of 2% (w/v) SDS. Bovine serum albumin was used as standard.

2.5. Enzymatic activity measurements

p-Nitrophenylphosphatase (p-NPPase) activity was assayed discontinuously at 37 °C in a Spectronic (Genesys 2) spectrophotometer by following the liberation of p-nitrophenolate ion (ε 1 M, pH 13 = 17,600 $M^{-1} \cdot cm^{-1}$), at 410 nm. Standard conditions were 50 mM AMPOL buffer, pH 10.0, containing 2 mM $MgCl_2$ and 1 mM p-NPP in a final volume of 1.0 mL, as previously described [30,31].

All determinations were carried out in duplicate and the initial velocities were constant for at least 90 min provided that less than 5% of substrate was hydrolyzed. Controls without added enzyme were included in each experiment to allow for the non-enzymatic hydrolysis of substrate. One enzyme unit (1 U) is defined as the amount of enzyme hydrolyzing 1.0 nmol of substrate per min at 37 °C per mL or mg of protein.

2.6. Solubilization of alkaline phosphatase with polyoxyethylene 9-lauryl ether

Membrane-bound alkaline phosphatase (0.02 mg·mL^{-1} of total protein) was solubilized with 1% polidocanol (w/v) (final concentration) for 1 h with constant stirring at 25 °C. After centrifugation at 100,000×*g* for 1 h at 4 °C, the solubilized enzyme was concentrated as described by Ciancaglini et al. [6]. To remove excess detergent, 1 mL of polidocanol-solubilized enzyme (~0.05 mg protien·mL^{-1}) was added to 200 mg of Calbiosorb resin as described by Camolezi et al. [32] and Simão et al. [13] and the suspension was mixed for 2 h at 4 °C. The supernatant is the source of detergent-free, solubilized enzyme.

2.7. Liposome preparation

DPPC, Chol, SM and GM1, in appropriate molar ratio, were dissolved in chloroform and dried under nitrogen flow. The resulting lipid film was kept under vacuum overnight and resuspended in 50 mM Tris–HCl buffer, pH 7.5, containing 2 mM $MgCl_2$. The mixture was incubated for 1 h at 60 °C, above the critical phase transition temperature of the lipid, and vortexed for each 10 min. Large unilamellar vesicles (LUVs) were prepared by submitting the suspension to extrusion (eleven times) through two 100 nm polycarbonate membranes in a LiposoFast extrusion system (Liposofast, Sigma-Aldrich). Binary systems constituted by DPPC:Chol, DPPC:SM and DPPC:GM1 (9:1) molar ratio; ternary systems constituted by DPPC:Chol:SM, DPPC:Chol:GM1 and DPPC:SM:GM1 (8:1:1) molar ratio and quaternary system constituted by DPPC:Chol:SM:GM1 (7:1:1:1), molar ratio, 10 mg·mL^{-1} final concentration, were prepared and used in the same day.

2.8. Incorporation of alkaline phosphatase into liposomes

Equal volumes of liposomes (10 mg·mL^{-1}) and TNAP (0.02 mg·mL^{-1}) resulting in a 1:10,000 protein:lipid ratio, in 50 mM Tris–HCl buffer, pH 7.5, containing 2 mM $MgCl_2$, were mixed and incubated at 25 °C during 1 h and the sample was centrifuged at 150,000×*g* for 20 min. The pellet was resuspended in 50 mM Tris–HCl buffer, pH 7.5, containing 2 mM $MgCl_2$, to the original volume. Was determined the percent of TNAP incorporation considering the enzymatic activity of the total sample before ultracentrifugation as 100% and comparing it with the enzymatic activity remaining in the supernatant (non-incorporated enzyme) after ultracentrifugation. By the difference between these values, it has the percent of protein incorporation in the proteoliposomes (pellet) [13].

2.9. Dynamic light scattering measurements (DLS)

The determination of liposomes size distribution was performed by DLS, using a N5 Submicron Particle Size Analyser (Beckman Coulter, Inc., Fullerton, CA, USA). Average value (n = 5) of the liposomes diameters was obtained at 25 °C by unimodal distribution, previously filtered (0.8 μm), as described by Bolean et al. [17].

2.10. Differential scanning calorimetry (DSC)

Transition phase temperatures (Tc) of the LUVs membranes prepared with different lipid compositions were studied by DSC. All LUVs suspensions and reference buffer employed in the experiment were previously degasified under vacuum (140 mbar) for 15 min.

The samples were scanned from 10 to 90 °C at an average heating rate of 0.5 °C·min^{-1} and the recorded thermograms were analyzed using a Nano-DSC II — Calorimetry Sciences Corporation, CSC (Lindon, Utah, USA). A minimum of at least three heating and cooling scans were performed for each analysis and all thermograms were reproducible. In order to ensure homogeneity in the analysis of the effect of the insertion of the enzyme and presence of different microdomains on the lipid phase transitions, we have chosen the simplest baseline correction to introduce the least amount of variability when comparing thermograms from different sets of experiments [17].

2.11. Estimation of lipids concentration

After extraction with chloroform: methanol (1:1 v/v), phospholipids and cholesterol composition of proteoliposomes or liposomes were quantified by the methods of Chen et al. [33] and Higgins [34], respectively. No significant variations (less 5%) were observed in the quantification of these lipids after and before extrusion.

3. Results and discussion

3.1. Production and biophysical characterization of ternary liposomes and proteoliposomes with microdomains constituted by DPPC:Chol enriched by SM and GM1

Liposomes constituted by DPPC:Chol (9:1), DPPC:Chol:SM (8:1:1) and DPPC:Chol:GM1 (8:1:1) (molar ratios) were evaluated by DLS and DSC and the resulting thermograms are presented in Fig. 1. All thermograms were analyzed by deconvolution for a better resolution of the existent distinct peaks in each case.

The average diameters are consistent with the membrane used in the extrusion method (100 nm) and low PI values were obtained for all liposome samples analyzed (Table 1).

As shown in Fig. 1A, DPPC:Chol (9:1) liposomes undergo lateral phase segregation, with the formation of cholesterol-rich domains

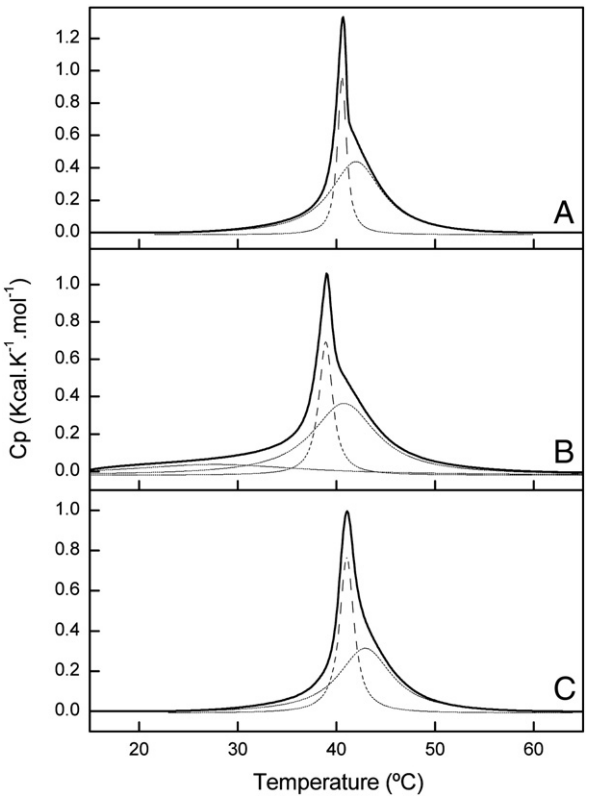

Fig. 1. DSC thermograms of liposomes (10 mg·mL^{-1}). Differential scanning calorimetry thermograms were processed in excess heat capacity, Cp (kcal·K^{-1}·mol^{-1}) as a function of temperature (°C) of liposomes constituted by: (A) DPPC:Chol (9:1), (B) DPPC:Chol:SM (8:1:1) and (C) DPPC:Chol:GM1 (8:1:1), molar ratio. Dashed curves symbolize deconvolution analysis.

Table 1
Thermodynamic parameters of liposomes (10 mg·mL^{-1}) constituted by DPPC, Chol, SM and GM1 with different lipid molar ratios.

Liposome composition	Lipid molar ratio	Diameter (nm)	PI	Peak	ΔH (kcal·mol^{-1})	T_c (°C)	$\Delta t_{1/2}$ (°C)
DPPC:Chol	9:1	175.5 ± 7.07	0.09 ± 0.08	1[a]	1.64	40.6	1.08
				2	4.52	42.0	6.37
DPPC:SM	9:1	168.4 ± 10.80	0.13 ± 0.11	1	0.91	29.0	8.02
				2[a]	8.89	40.0	2.20
DPPC:GM1	9:1	178.5 ± 8.09	0.95 ± 0.08	1	9.33	41.5	2.29
DPPC:Chol:SM	8:1:1	146.1 ± 10.8	0.10 ± 0.04	1	2.29	27.8	23.52
				2[a]	1.87	38.9	1.66
				3	4.79	40.8	7.98
DPPC:Chol:GM1	8:1:1	169.6 ± 13.02	0.27 ± 0.12	1[a]	2.12	41.1	1.75
				2	3.30	42.9	6.51
DPPC:SM:GM1	8:1:1	245.7 ± 18.25	0.72 ± 0.23	1	8.42	40.5	3.70
DPPC:Chol:SM:GM1	7:1:1:1	151.5 ± 21.94	0.12 ± 0.46	1[a]	2.54	39.1	2.88
				2	4.20	42.3	7.82

[a] Principal transition.

(T_C = 42.0 °C) and cholesterol-poor domains (T_C = 40.6 °C) on the membrane, in agreement with previous studies [17].

The insertion of SM in the DPPC:Chol system provided a considerable broadening on the peaks as shown in Fig. 1B, increasing the $\Delta t_{1/2}$ values (Table 1), evidencing a decrease in phase transition cooperativity. Furthermore, a large centered transition in Tc = 27.8 °C was observed in the thermogram, possibly related to the SM or DPPC pre-transition. The total enthalpy (8.95 kcal·mol^{-1}) of the DPPC:Chol:SM system increased in relation to the DPPC:Chol (6.16 kcal·mol^{-1}) binary system. This effect can be explained by the geometry of the SM molecule, capable of stabilizing the membrane through the hydrogen bridges interactions between the hydrocarbon chains.

It is known that the membrane's cholesterol and sphingomyelin clustering differentiate from the DPPC:Chol constituted membranes [35–37]. The compressibility of membranes containing SM/Chol was in fact much better than in membranes constituted by DPPC with equal cholesterol concentration [35–37]. Moreover, water permeability was lower in SM/Chol than in DPPC/Chol, indicating the formation of a more efficient clustering and/or increase in permeability could be due to phase coexistence [38].

Natural SM normally constitutes a populational mixture with amide-bonds of the hydrocarbon chain differentiating in width and length (from 16 to 24 carbons) [39]. The hydrocarbon chain composition of the SM varies among the tissues, however, the presence of exceptionally long chains is common, giving the molecule a natural asymmetry. PCs normally have moderately long hydrocarbon chains (16–18 carbons) with lengths approximately the same [40].

GM1 are generally found in higher concentrations in the brain, whereas present in many types of cells and are known for residing exclusively in the extracellular monolayer of biological membranes [41]. In systems used as membrane models, such as unilamellar vesicles, it was shown that GM1 distribute themselves between surfaces of the monolayers. However, its distribution between the two membrane leaflets is not equal [42,43].

In contrast to cholesterol, it is known that GM1, when added to DPPC-constituted vesicles, does not undergo lateral phase segregation [44,45]. As can be seen in Fig. 1C, the lateral phase segregation with a peak centered at a higher Tc (42.9 °C) than the characteristic DPPC Tc (41.5 °C) relates to cholesterol-rich microdomains. In this case, the presence of GM1 in the ternary systems influences mainly ΔH and the phase transition cooperativity (Table 1).

DSC and X-ray diffraction studies show that bovine brain GM1, with low hydration, exhibits a wide thermal transition and forms a cylindrical hexagonal phase instead of bilayer [46]. Aqueous dispersions with gangliosides and egg yolk PC were examined using electronic microscopy; lamellar structures were observed in low concentrations of gangliosides (<30%), spherical micelles in high concentrations of gangliosides (>80%) and cylindrical structures in the 45:48% GM1:DPPC ratio respectively. This suggests that the cylindrical structure represented an intermediary in the conversion of the lamellar phase to the micellar phase [47]. It is important to point out that the DSC curves obtained for GM1 presented in literature [48], alone or in vesicular systems in the presence of DPPC, are difficult to compared, since they have shown very wide transition peaks besides being obtained with very high heating and cooling velocities, which contributes to a loss in measurement quality.

TNAP was incorporated to liposomes forming proteoliposomes of binary and ternary lipid mixtures. In the proteoliposome's thermogram constituted by DPPC:Chol (9:1) (Fig. 2A) the lateral phase

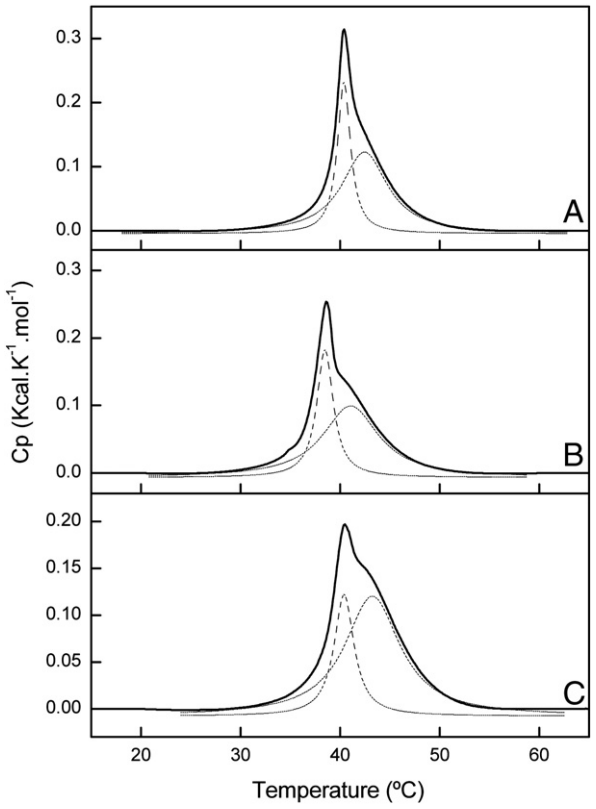

Fig. 2. DSC thermograms of proteoliposomes (10 mg·mL^{-1}). Differential scanning calorimetry thermograms were processed in excess heat capacity, Cp (kcal·K^{-1}·mol^{-1}) as a function of temperature (°C) of liposomes constituted by: (A) DPPC:Chol (9:1), (B) DPPC:Chol:SM (8:1:1) and (C) DPPC:Chol:GM1 (8:1:1), molar ratio. Dashed curves symbolize deconvolution analysis.

segregation can be noted. Since the same profile was detected for liposomes with the same composition, it proves that the enzyme is not capable of influencing the calorimetric profile of this system; however, the thermodynamic parameters are significantly altered. Comparing the thermodynamic parameter values of the liposomes shown on Table 1 with the proteoliposomes parameters from Table 2, an intense decrease in total ΔH can be observed, demonstrating how much the enzyme can fluidify the system.

Tc values were not significantly altered. Regarding cooperativity (Table 2), it can be noted that the first centered peak at 40 °C becomes a little wider, however, the second peak centered at 42 °C becomes slightly more cooperative. The TNAP reconstitution in DPPC:Chol liposomes yielded a 62.1% incorporation of the catalytic activity.

In Fig. 2B and C the thermogram profiles for the ternary proteoliposomes constituted by DPPC:Chol:SM and DPPC:Chol:GM1 (8:1:1) molar ratio, respectively, can be observed. In the first case we see that, in the presence of the enzyme the peak referring to the pre-transition is eliminated. In the second case, the profile stays very similar when compared to the liposome system, yet the peak distinction is more evident when the enzyme is present. Comparing the thermodynamic parameters, the presence of the enzyme fluidifies the systems, with a decrease in ΔH values of the proteoliposomes compared to the liposomes.

The TNAP reconstitution in DPPC:Chol:SM and DPPC:Chol:GM1 liposomes yielded an incorporation of around 30% of the enzymatic activity, demonstrating that the presence of SM and GM1 has a negative effect in the enzyme incorporation when compared to the values obtained for the proteoliposomes in the presence of cholesterol.

The spontaneous insertion of AP in lipid ordered domains was visualized using AFM, which supports the preference of GPI-anchored proteins for the lipid bilayer area in which lipid clustering is tight [27].

3.2. Production and biophysical characterization of binary liposomes and proteoliposomes constituted by DPPC:SM and DPPC:GM1

Next, we studied binary vesicles in the absence of cholesterol to examine the thermotropic behavior of SM and GM1 alone. For that purpose, DPPC:SM and DPPC:GM1 (9:1) molar ratio constituted liposomes were used (Fig. 3). Deconvolution analysis enable the detection of a pre-transition centered at Tc = 20.0 °C and a main transition peak at Tc = 40.0 °C (Fig. 3), in agreement with earlier studies [49,50].

SM and PC have regularly cylindrical molecular forms, forming bilayers when hydrated to minimize free energy [51]. Nevertheless, SM exhibits a more complex behavior than PC in membranes [39,49,52]. SMs with saturated hydrocarbon chains with a length of 16 to 24 carbons have a main transition between 37 and 48 °C, with an increase in temperature, although not linear, with the increase in the carbon chain [52]. Tc values for SM are normally less affected by the cis-insaturation insertion in the carbon chain when compared to other

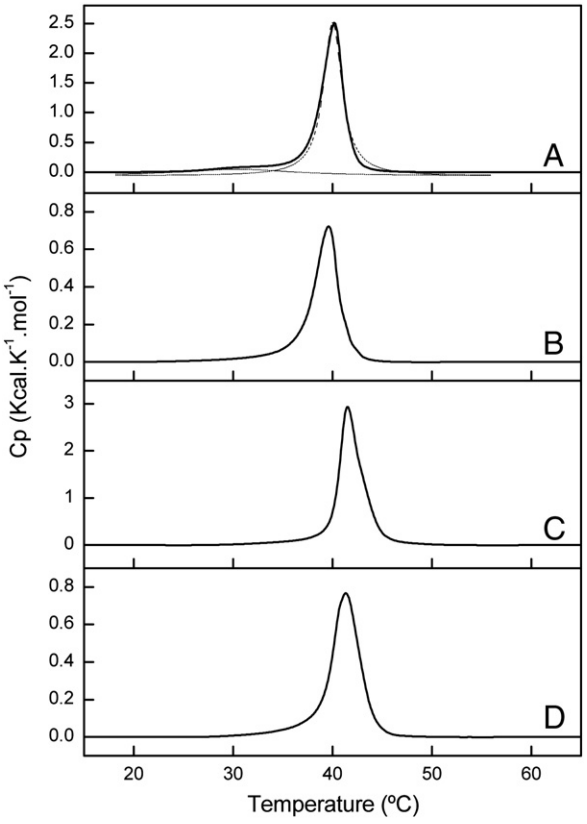

Fig. 3. DSC thermograms of binary systems without cholesterol (10 mg·mL^{-1}). Differential scanning calorimetry thermograms were processed in excess heat capacity, Cp (kcal·K^{-1}·mol^{-1}) as a function of temperature (°C) of vesicles constituted by: (A) DPPC:SM (9:1) liposome, (B) DPPC:SM (9:1) proteoliposome, (C) DPPC:GM1 (9:1) liposome and (D) DPPC:GM1 (9:1) proteoliposome, molar ratio. Dashed curves symbolize deconvolution analysis.

phospholipids. The phenomenon was attributed to the bilayer stabilization by hydrogen bonds [52].

Through the data from Table 1 it is possible to notice a significant increase in the ΔH value for the DPPC:SM liposomes value (8.89 kcal·mol^{-1}) in relation to the DPPC:Chol liposomes (ΔH_{total} = 6.16 kcal·mol^{-1}). This fact demonstrates that the SM molecule geometry is capable of stabilizing the DPPC molecule. This more efficient lipid packing can be in part explained by a better attraction of the van der Waals force between the saturated hydrocarbon chains and the DPPC.

The addition of GM1 to the DPPC vesicles was not able to affect the characteristic Tc of DPPC, showing evidence of just a slight broadening

Table 2
Thermodynamic parameters of proteoliposomes (10 mg·mL^{-1}) constituted by DPPC, Chol, SM and GM1 with different lipid molar ratios.

Proteoliposome composition	Lipid molar ratio	Incorporation (%)	Diameter (nm)	PI	Peak	ΔH (kcal·mol^{-1})	T_c (°C)	$\Delta t_{1/2}$ (°C)
DPPC:Chol	9:1	62.1	132.7 ± 8.75	0.11 ± 0.05	1[a]	0.58	40.4	1.59
					2	1.17	42.4	5.75
DPPC:SM	9:1	21.9	133.1 ± 9.10	0.09 ± 0.06	1	2.71	39.6	2.60
DPPC:GM1	9:1	17.9	145.8 ± 20.43	0.29 ± 0.18	1	3.01	41.4	2.87
DPPC:Chol:SM	8:1:1	30.2	136.3 ± 21.87	0.12 ± 0.11	1[a]	0.56	38.6	1.93
					2	1.24	41.0	7.18
DPPC:Chol:GM1	8:1:1	30.6	127.5 ± 18.63	0.22 ± 0.12	1[a]	0.45	40.4	2.32
					2	1.48	43.1	7.11
DPPC:SM:GM1	8:1:1	27.6	140.7 ± 21.89	0.27 ± 0.16	1	2.11	40.5	5.00
DPPC:Chol:SM:GM1	7:1:1:1	25.6	113.1 ± 15.54	0.25 ± 0.21	1	0.45	38.2	4.10
					2[a]	1.41	42.0	8.37

[a] Principal transition.

of the peak with decrease of cooperativity in the system phase transition (Fig. 3C and Table 1).

These data can be related with the results found by Reed and Shipley [48], which shows a small effect on Tc and broadening of the DPPC phase transition peak with and addition of up to 9.5% mol in GM1. In addition to that, we observed that the presence of GM1 was capable of increasing ΔH, thus making the vesicle systems more packed (Table 1).

It is important to note that lateral phase segregation was not detected in any of the thermograms (DPPC:SM and DPPC:GM1), under these conditions. Hence, cholesterol is likely responsible for this effect when two distinct peaks are observed in the thermograms referring to the ternary systems.

We can emphasize then that the DSC technique is an efficient method to study the microdomains formation and the changes in thermodynamic parameters caused by the different lipid compositions. Furthermore, this technique can give us an idea of the presence of the enzyme in membrane model systems. This method does not require the use of probes that might disturb the system. It is also insensitive to the size of the domain. Thus, the evidence of the presence of small domains, not resolvable with light microscopy, can be obtained [53].

As seen in Fig. 3B, the presence of the enzyme in proteoliposomes thermogram constituted by DPPC:SM (9:1), the peak related to the pre-transition is eliminated.

Regarding the DPPC:GM1 (9:1) (Fig. 3D) proteoliposomes, the enzyme is not capable of influencing the calorimetric profile of this system, but the thermodynamic parameters are expressively altered. By comparing the thermodynamic parameters of the liposomes presented on Table 1 with the proteoliposome's parameters from Table 2, we have a significant decrease in total ΔH values, demonstrating how much the enzyme can fluidify the system. Cooperativity is slightly affected with a small widening of the peaks (Table 2).

In the TNAP reconstitution studies in DPPC:SM and DPPC:GM1 liposomes around 20% incorporation of catalytic activity was obtained, demonstrating a negative effect even greater in the enzyme incorporation when compared to the values obtained for the DPPC:Chol constituted proteoliposomes.

Sesana et al. [54] have shown a reduction in hydrolysis Vmax of alkaline phosphatase in the presence of Chol and SM in proteoliposomes constituted by a PC matrix. Moreover, there was an increase in liposomes diameters. The presence of GM1, however, has provided a small increase in hydrolysis Vmax and did not significantly alter liposome diameters.

3.3. Production and biophysical characterization of ternary liposomes and proteoliposomes with microdomains constituted by DPPC:SM:GM1

To better understand these data, it was necessary to perform studies involving ternary systems constituted by DPPC:SM:GM1 (8:1:1 molar ratio), that is, in the absence of Chol, in order to perceive the consequences of the interactions of SM and GM1. The average diameter data and polydispersion values are shown on Table 1 for the liposome systems as on Table 2 for the proteoliposomes systems.

The calorimetric profile of this liposome is shown on Fig. 4, where one can observe the elimination of the pre-transition characteristic peak, centered around 29 °C, which is present on the thermogram obtained for the DPPC:SM (9:1) liposomes.

Lateral phase segregation was not detected for this system, thus confirming that the SM and GM1 interactions, in these conditions, also do not cause the existence of microdomains rich in certain compounds.

Through the data from Table 1 it is possible to see a high ΔH value for the liposomal system (8.42 kcal·mol^{-1}), demonstrating once more that the geometry of the SM and GM1 molecules stabilize the DPPC constituted membrane, making the clustering among lipids more efficient.

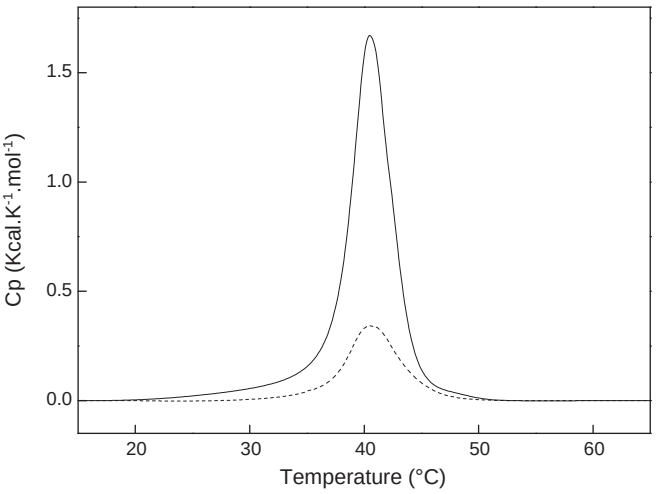

Fig. 4. DSC thermograms of ternary systems without cholesterol (10 mg·mL^{-1}). Differential scanning calorimetry thermograms were processed in excess heat capacity, Cp (kcal·K^{-1}·mol^{-1}) as a function of temperature (°C) of vesicles constituted by DPPC:SM:GM1 (8:1:1), molar ratio: (—) liposome and (— — —) proteoliposome.

The three ternary systems, present very similar Tc, from 40 to 41 °C (Table 1). Furthermore, these systems present enlarged peaks with high $\Delta t_{1/2}$ values.

In Fig. 4, the sharp decrease in ΔH values by the presence of the enzyme in the vesicular system becomes more evident. Its presence does not significantly influence Tc and decreases cooperativity with the increase in $\Delta t_{1/2}$ value (Table 2).

The TNAP reconstitution in DPPC:SM:GM1 liposomes has provided around 30% incorporation of the catalytic activity (Table 2). These data demonstrate a negative effect very similar among ternary systems.

3.4. Production and biophysical characterization of quaternary liposomes and proteoliposomes with microdomains constituted by DPPC:Chol:SM:GM1

In conclusion, studies aiming to increase the complexity of the system were performed with the objective to approximate our mimetic systems to the existent microdomains in biological membranes, the so called “lipid rafts”. Thus, DPPC:Chol:SM:GM1 (7:1:1:1 molar ratio) constituted liposomes were formed in the same conditions mentioned above.

The calorimetric profile of the liposome and proteoliposomes systems is in Fig. 5. With the deconvolution analysis, the presence of microdomains rich in cholesterol can be observed, characterized by the second peak centered at 42.3 °C (Fig. 5A). This Tc values is very similar to the one found for binary and ternary systems where cholesterol is present, this being another strong evidence that this transition is related to the lateral phase transition induced by the sterol. This phase segregation is even more pronounced when the enzyme is present in the system (Fig. 5B), since the second peak area centered at 42 °C becomes more resolved (Table 2), showing a higher ΔH (1.41 kcal·mol^{-1}) value.

Regarding Tc, the main transition peak as well as the peak relating to the microdomains rich in cholesterol, for the liposome and proteoliposomes, are very similar. In a previous work in our research group, Bolean et al. [17] have compared the calorimetric profile of three different systems: DPPC-liposome, DPPC-proteoliposomes and DPPC-proteoliposomes after TNAP cleavage using PIPLC. This study shows that the alterations related to the proteoliposome system fluidity are related mainly to the GPI anchor insertion.

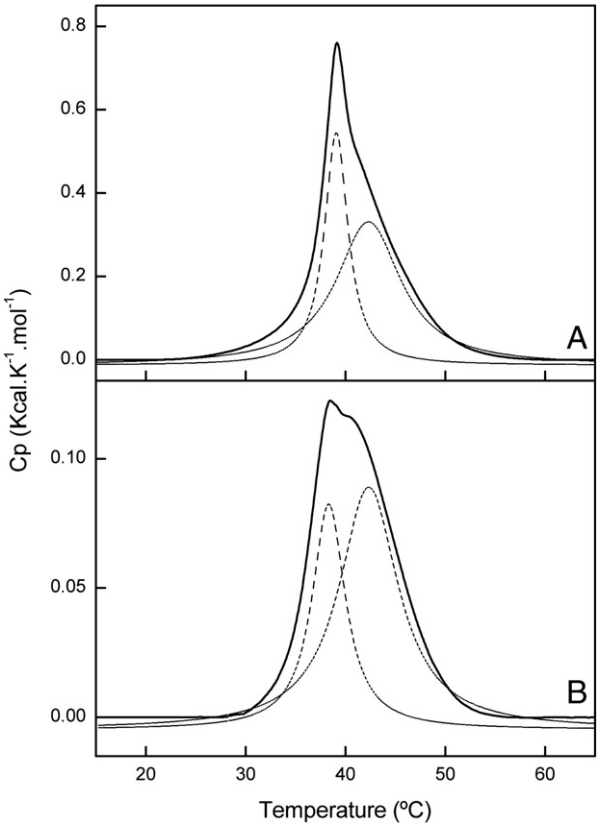

Fig. 5. DSC thermograms of quaternary systems (10 mg·mL^{-1}). Differential scanning calorimetry thermograms were processed in excess heat capacity, Cp (kcal·K^{-1}·mol^{-1}) as a function of temperature (°C) of vesicles constituted by DPPC:Chol:SM:GM1 (7:1:1:1), molar ratio: (A) Liposome and (B) Proteoliposome. Dashed curves symbolize deconvolution analysis.

The quaternary liposome presents a phase transition with a high $\Delta t_{1/2}$ value and low cooperativity and this broadening is even greater in the presence of the enzyme (Table 2). The TNAP reconstitution in such system resulted in around 25% incorporation of catalytic activity. This was one of the smallest percentage value among all the systems studied, showing that the association of the four components induces a greater negative effect in the enzyme incorporation.

4. Conclusions

In summary, with the increase of the lipid components in the membrane models, even more complex models can be formed with the presence of lipid microdomains. Due to the favorable molecular interactions between the lipid rafts components, direct insertion of the enzyme via its GPI anchor is observed but with smaller percentages of enzyme incorporation. Thus, the strategy of enzyme incorporation into liposome with complex compositions via direct insertion results in low yield of incorporation.

The already formed liquid-ordered complexes in the liposomes are presented with a greater lipid packing when compared to other regions of the membrane surface. Because of this, the posterior insertion of the enzyme into these microdomains was difficult. On the other hand, these systems are excellent for the study of changes in the enzyme catalytic activity in the presence of different lipids in model membranes.

In general, the presence of TNAP in proteoliposomes caused a reduction in ΔH values when compared to the systems without the protein. Furthermore, there was a reduction in cooperativity, but changes in T_C were not detected. In some cases, the presence of the enzyme resulted in an even greater segregation of the different phase transition peaks.

The relevance of the results described in this study encourages us to carry out further biophysical studies with membrane models that better mimic MVs. The results also encourage studies about the kinetic behavior of TNAP in the presence of different lipid microdomains. This can contribute to the overall understanding of the roles of lipids and their interactions with TNAP during the biomineralization process.

Acknowledgements

The authors thank Priscila Cerviglieri for the linguistic advice. We also thank FAPESP, CAPES and CNPq for the financial support given to our laboratory. MB, AMSS and BZF received a CAPES, FAPESP and CNPq scholarship, respectively.

References

[1] G.W. Cyboron, R.E. Wuthier, Purification and initial characterization of intrinsic membrane-bound alkaline phosphatase from chicken epiphyseal cartilage, J. Biol. Chem. 256 (1981) 7262–7268.
[2] R.E. Wuthier, J.E. Chin, J.E. Hole, T.C. Register, Y.H. Laura, Y. Ishikawa, Isolation and characterization of calcium accumuling matrix vesicles from chondrocytes of chicken epiphsyeal growth plate cartilage in primary culture, J. Biol. Chem. 260 (1985) 15972–15979.
[3] C. Curti, J.M. Pizauro, G. Rossinholi, I. Vugman, J.A. Mello de Oliveira, F.A. Leone, Isolation and kinetic properties of an alkaline phosphatase from rat bone matrix-induced cartilage, Cell. Mol. Biol. 32 (1986) 55–62.
[4] J.C. Say, K. Ciuffi, R.P.M. Furriel, P. Ciancaglini, F.A. Leone, Alkaline phosphatase from rat osseous plates: purification and biochemical characterization of a soluble form, Biochim. Biophys. Acta 1074 (1991) 256–262.
[5] F.A. Leone, J.M. Pizauro, P. Ciancaglini, Rat osseous plate alkaline phosphatase: a search for its role in biomineralization, Trends in Comparative Biochem. Physiol. 3 (1997) 57–73.
[6] P. Ciancaglini, A.M.S. Simão, F.L. Camolezi, J.L. Millán, J.M. Pizauro, Contribution of matrix vesicles and alkaline phosphatase to ectopic bone formation, Braz. J. Med. Biol. Res. 39 (2006) 603–610.
[7] J.L. Millán, Mammalian Alkaline Phosphatase: From Biology to Applications in Medicine and Biotechnology, Wiley-VCH Verlag GmbH & Co, KGaA, Weinheim, 2006.
[8] A. Mota, P. Silva, D. Neves, C. Lemos, C. Calhau, D. Torres, F. Martel, H. Fraga, L. Ribeiro, M.N.M.P. Alçada, M.J. Pinho, M.R. Negrão, R. Pedrosa, S. Guerreiro, J.T. Guimarães, I. Azevedo, M.J. Martins, Characterization of rat heart alkaline phosphatase isoenzymes and modulation of activity, Braz. J. Med. Biol. Res. 41 (2008) 600–609.
[9] H. Orimo, The mechanism of mineralization and the role of alkaline phosphatase in health and disease, J. Nippon Med. Sch. 77 (2010) 4–12.
[10] J.M. Pizauro, P. Ciancaglini, F.A. Leone, Characterization of the phosphatidylinositol-specific phospholipase C-released form of rat osseous plate alkaline phosphatase and its possible significance on endochondral ossification, Mol. Cel. Biochem. 152 (1995) 121–129.
[11] H.C. Anderson, J.B. Sipe, L. Hessle, R. Dhamyamraju, E. Atti, N.P. Camacho, J.L. Millán, Impaired calcification around matrix vesicles of growth plate and bone in alkaline phosphatase-deficient mice, Am. J. Pathol. 164 (2004) 841–847.
[12] P. Ciancaglini, M.C. Yadav, A.M.S. Simão, S. Narisawa, J.M. Pizauro, C. Farquharson, M.F. Hoylaerts, J.L. Millán, Kinetic analysis of substrate utilization by native and TNAP-, NPP1- or PHOSPHO1-deficient matrix vesicles, J. Bone Miner. Res. 25 (2010) 716–723.
[13] A.M. Simão, M.C. Yadav, S. Narisawa, M. Bolean, J.M. Pizauro, M.F. Hoylaerts, P. Ciancaglini, J.L. Millán, Proteoliposomes harboring alkaline phosphatase and nucleotide pyrophosphatase as matrix vesicle biomimetics, J. Biol. Chem. 285 (2010) 7598–7609.
[14] A.M. Simão, M.C. Yadav, P. Ciancaglini, J.L. Millán, Proteoliposomes as matrix vesicles' biomimetics to study the initiation of skeletal mineralization, Braz. J. Med. Biol. Res. 43 (2010) 234–241.
[15] L.N. Wu, Y. Guo, B.R. Genge, Y. Ishikawa, R.E. Wuthier, Transport of inorganic phosphate in primary cultures of chondrocytes isolated from the tibial growth plate of normal adolescent chickens, J. Cell. Biochem. 86 (2002) 475–489.
[16] M. Eddin, The state of lipid rafts: from model membrane to cell, Annu. Rev. Biophys. Biomol. Struct. 32 (2003) 257–283.
[17] M. Bolean, A.M.S. Simão, B.Z. Favarin, J.L. Millán, P. Ciancaglini, The effect of cholesterol on the reconstitution of alkaline phosphatase into liposomes, Biophys. Chem. 152 (2010) 74–79.
[18] D.A. Brown, E. London, Structure and function of sphingolipid- and cholesterol-rich membrane rafts, J. Biol. Chem. 275 (2000) 17221–17224.
[19] K. Simons, D. Toomre, Lipid rafts and signal transduction, Nat. Rev. Mol. Cell Biol. 1 (2000) 31–39.
[20] D. Lingwood, K. Simons, Lipid rafts as a membrane-organizing principle, Science 327 (2010) 46–50.
[21] K. Simons, E. Ikonen, Functional rafts in cell membranes, Nature 387 (1997) 569–572.

[22] C. Dietrich, L.A. Bagatolli, Z.N. Volovyk, N.L. Thompson, M. Levi, K. Jacobson, E. Gratton, Lipid rafts reconstituted in model membranes, Biophys. J. 8 (2001) 1417–1428.
[23] D. Lichtenberg, F.M. Goñi, H. Heerklotz, Detergent-resistant membranes should not be identified with membrane rafts, Trends Biochem. Sci. 30 (2005) 430–436.
[24] P.L. Yeagle, The Membranes of Cells, Second Edition Academic Press, INC, 2004.
[25] A. Kouzayha, F. Besson, GPI-alkaline phosphatase insertion into phosphatidylcholine monolayers: phase behavior and morphology changes, Biochem. Biophys. Res. Commun. 333 (2005) 1315–1321.
[26] M.C. Giocondi, F. Besson, P. Dosset, P.E. Milhiet, C. Le Grimellec, Temperature-dependent localization of GPI-anchored intestinal alkaline phosphatase in model rafts, J. Mol. Recognit. 20 (2007) 531–537.
[27] P.E. Milhiet, M.C. Giocondi, O. Baghdadi, F. Ronzon, B. Roux, C. Le Grimellec, Spontaneous insertion and partitioning of alkaline phosphatase into model lipid rafts, EMBO Rep. 3 (2002) 485–490.
[28] M. Didier, P.E. Lenne, H. Rigneault, H.T. He, Dynamic of the plasma membrane: how to combine fluidity and order, EMBO J. 25 (2006) 3446–3457.
[29] E.F. Hartree, Determination of protein: a modification of the Lowry method that gives a linear photometric response, Anal. Biochem. 48 (1972) 422–427.
[30] A.M.S. Simão, M.M. Beloti, R.M. Cezarino, A.L. Rosa, J.M. Pizauro, P. Ciancaglini, Membrane-bound alkaline phosphatase from ectopic mineralization and rat bone marrow cell culture, Comp. Biochem. Physiol. A Mol. Integr. Physiol. 146 (2007) 679–687.
[31] A.M.S. Simão, M.M. Beloti, A.L. Rosa, P.T. de Oliveira, J.M. Granjeiro, J.M. Pizauro, P. Ciancaglini, Culture of osteogenic cells from human alveolar bone: a useful source of alkaline phosphatase, Cell Biol. Int. 31 (2007) 1405–1413.
[32] F.L. Camolezi, K.R.P. Daghastanli, P.P. Magalhães, J.M. Pizauro, P. Ciancaglini, Construction of an alkaline phosphatase–liposome system: a tool for biomineralization study, Int. J. Biochem. Cell Biol. 34 (2002) 1091–1101.
[33] P.S. Chen Jr., T.Y. Toribara, H. Warner, Microdetermination of phosphorus, Anal. Chem. 28 (1956) 1756–1758.
[34] G. Higgins, Separation and analysis of membrane lipid components, in: J.B.C. Findlay, W.H. Evans (Eds.), Biological Membranes (Practical Approach series), IRL Press Oxford, Washington, DC, 1987, pp. 104–137.
[35] X.M. Li, M.M. Momsen, J.M. Smaby, H.L. Brockman, R.E. Brown, Cholesterol decreases the interfacial elasticity and detergent solubility of sphingomyelins, Biochemistry 40 (2001) 5954–5963.
[36] B. Snyder, E. Freire, Compositional domain structure in phosphatidylcholine-cholesterol and sphingomyelin-cholesterol bilayers, Proc. Natl. Acad. Sci. U.S.A. 77 (1980) 4055–4059.
[37] D. Needham, R.S. Nunn, Elastic deformation and failure of lipid bilayer membranes containing cholesterol, Biophys. J. 58 (1990) 997–1009.
[38] M. Fidorra, L. Duelund, C. Leidy, A.C. Simonsen, L.A. Bagatolli, Absence of fluid-ordered/fluid-disordered phase coexistence in ceramide/POPC mixtures containing cholesterol, Biophys. J. 90 (2006) 4437–4451.
[39] Y. Barenholz, in: M. Shinitzky (Ed.), Physiology of Membrane Fluidity, 1, CRC Press, Boca Raton, FL, 1984, pp. 131–173.
[40] A.H. Merrill Jr., E.M. Schmelz, D.L. Dillehay, S. Spiegel, J.A. Shayman, J.J. Schroeder, R.T. Riley, K.A. Voss, E. Wang, Sphingolipids — the enigmatic lipid class: biochemistry, physiology, and pathophysiology, Toxicol. Pharmacol. 142 (1997) 208–225.
[41] P.H. Fishman, R.O. Brady, Biosynthesis and function of gangliosides, Science 194 (1976) 906–915.
[42] B. Cestaro, Y. Barenholz, S. Gatt, Hydrolysis of di- and trisialo gangliosides in micellar and liposomal dispersion by bacterial neuraminidases, Biochemistry 19 (1980) 615–619.
[43] B. Maggio, G.G. Montich, F.A. Cumar, Surface topography of sulfatide and gangliosides in unilamellar vesicles of dipalmitoylphosphatidylcholine, Chem. Phys. Lipids 46 (1988) 137–146.
[44] L.O. Sillerud, D.E. Schafer, R.K. Yu, W.H. Konigsberg, Calorimetric properties of mixtures of ganglioside GM1 and dipalmitoylphosphatidylcholine, J. Biol. Chem. 254 (1979) 10876–10880.
[45] M. Masserini, E. Freire, Thermotropic characterization of phosphatidylcholine vesicles containing ganglioside GM1 with homogeneous ceramide chain length, Biochemistry 25 (1986) 1043–1049.
[46] W. Curatolo, D.M. Small, G.G. Shipley, Phase behavior and structural characteristics of hydrated bovine brain gangliosides, Biochim. Biophys. Acta 468 (1977) 11–20.
[47] M.W. Hill, R. Lester, Mixtures of gangliosides and phosphatidylcholine in aqueous dispersions, Biochim. Biophys. Acta 282 (1972) 18–30.
[48] R.A. Reed, G.G. Shipley, Properties of ganglioside GM1 in phosphatidylcholine bilayer membranes, Biophys. J. 70 (1996) 1363–1372.
[49] L.K. Bar, Y. Barenholz, T.E. Thompson, Effect of sphingomyelin composition on the phase structure of phosphatidylcholine–sphingomyelin bilayers, Biochemistry 36 (1997) 2507–2516.
[50] B. Ramstedt, J.P. Slotte, Comparison of the biophysical properties of racemic and d-erythro-N-acyl sphingomyelins, Biophys. J. 77 (1999) 1498–1506.
[51] D. Marsh, General features of phospholipid phase transitions, Chem. Phys. Lipids 57 (1991) 109–120.
[52] R.D. Koynova, M. Caffrey, Phases and phase transitions of the sphingolipids, Biochim. Biophys. Acta 1255 (1995) 213–236.
[53] R.M. Epand, Detecting the presence of membrane domains using DSC, Biophys. Chem. 126 (2007) 197–200.
[54] S. Sesana, F. Re, A. Bulbarelli, D. Salerno, E. Cazzaniga, M. Masserini, Membrane features and activity of GPI-anchored enzymes: alkaline phosphatase reconstituted in model membranes, Biochemistry 47 (2008) 5433–5440.